Inorg. Chem. **2007**, *46*, 4090–4102

Synthesis and Structures of Bis(dithiolene)tungsten(IV,VI) Thiolate and Selenolate Complexes: Approaches to the Active Sites of Molybdenum and Tungsten Formate Dehydrogenases

Stanislav Groysman and R. H. Holm*

Department of Chemistry and Chemical Biology, Harvard University, Cambridge, Massachusetts 02138

Received December 20, 2006

Formate dehydrogenases are molybdenum- or tungsten-containing enzymes that catalyze the oxidation of formate to carbon dioxide. Among the significant characteristics of the mononuclear active sites are coordination of two pyranopterindithiolene ligands and selenocysteinate to the metal in oxidation states IV–VI. The first detailed investigation of the synthesis and structures of bis(dithiolene)tungsten selenolate and analogous thiolate complexes of relevance to formate dehydrogenases has been undertaken. Some 17 complexes of the types $[W^{IV}(QR)(S_2C_2Me_2)_2]^-$, $[W^{VI}O(QR)(S_2C_2Me_2)_2]^-$, and $[W^{VI}S(QR)(S_2C_2Me_2)_2]^-$ (Q = S, Se; R = *tert*-butyl, 1-adamantyl) and the desoxo species $[W^{VI}(SR)(OSiR'_3)(S_2C_2Me_2)_2]$ (R′ = Me, Ph) were prepared. Ten structures of representative members of these types were determined; W^{IV} complexes are square-pyramidal and W^{VI} complexes are six-coordinate, with geometries intermediate between octahedral and trigonal-prismatic. Selenolate complexes are less stable than similar thiolate species; decomposition products were identified as $[W^{V}_2(\mu_2\text{-}Q)_2(S_2C_2Me_2)_2]^{2-}$ and $[W^{IV,V}_2(\mu_2\text{-}Se)(S_2C_2Me_2)_4]^-$. The several $[Mo^{IV}(QR)(S_2C_2Me_2)_2]^-$ complexes prepared earlier and the tungsten compounds synthesized in this work form a family of molecules whose overall stereochemistry and metric features are those expected in the absence of protein structural constraints.

Introduction

As part of our elaboration of the synthetic, structural, and reactivity analogues of the mononuclear active sites of molybdenum and tungsten enzymes,[1] we have turned our attention to formate dehydrogenases (FDHs[2]). These enzymes have been purified from eukaryotes, archaea, and bacteria and catalyze the reaction $HCO_2^- = CO_2 + H^+ + 2e^-$.[3−6] Although not an oxotransferase, FDH has been classified in the DMSOR family.[3] FDHs are most frequently encountered as molybdoenzymes. The active site structures of FDHs obtained from protein crystallography[7−10] and extended X-ray absorption fine structure (EXAFS) analyses[11,12] are schematically summarized in Figure 1, where it is seen that all but one refer to Mo−FDHs. It is now apparent, long after their recognition in 1973−1983,[13,14] that a substantial number of W−FDHs exist.[15−19] In considering currently known FDH

* To whom correspondence should be addressed. E-mail: holm@chemistry.harvard.edu.

(1) Enemark, J. H.; Cooney, J. J. A.; Wang, J.-J.; Holm, R. H. *Chem. Rev.* **2004**, *104*, 1175−1200.
(2) Abbreviations: Ad = adamantyl; Ar = 2,4,6-$Pr^i_3C_6H_2$; bdt = benzene-1,2-dithiolate(2−); Bu^t_3tach = 1,3,5-tri-*tert*-butyl-1,3,5-triazacyclohexane; DMSOR = dimethyl sulfoxide reductase; FDH = formate dehydrogenase; Me_3tacn = 1,4,7-trimethyl-1,4,7-triazacyclononane; mnt = maleonitriledithiolate(2−); Q = O, S, Se; Tp* = tris(3,5-dimethylpyrazolyl)hydroborate(1−)
(3) Hille, R. *Chem. Rev.* **1996**, *96*, 2757−2816.
(4) Vorholt, J. A.; Thauer, R. K. *Met. Ions Biol. Syst.* **2002**, *39*, 571−619.
(5) Jormakka, M.; Byrne, B.; Iwata, S. *Curr. Opin. Struct. Biol.* **2003**, *13*, 418−423.
(6) Moura, J. J. G.; Brondino, C. D.; Trincâo, J.; Româo, M. J. *J. Biol. Inorg. Chem.* **2004**, *9*, 791−799.
(7) Boyington, J. C.; Gladyshev, V. N.; Khangulov, S. V.; Stadtman, T. C.; Sun, P. D. *Science* **1997**, *275*, 1305−1308.
(8) Raaijmakers, H. C. A.; Romão, M. J. *J. Biol. Inorg. Chem.* **2006**, *11*, 849−854.
(9) Jormakka, M.; Törnroth, S.; Byrne, B.; Iwata, S. *Science* **2002**, *295*, 1863−1868.
(10) Raaijmakers, H.; Macieira, S.; Dias, J. M.; Texeira, S.; Bursakov, S.; Huber, R.; Moura, J. J. G.; Moura, I.; Romão, M. J. *Structure* **2002**, *10*, 1261−1272.
(11) George, G. N.; Colangelo, C. M.; Dong, J.; Scott, R. A.; Khangulov, S. V.; Gladyshev, V. N.; Stadtman, T. C. *J. Am. Chem. Soc.* **1998**, *120*, 1267−1273.
(12) George, G. N.; Costa, C.; Moura, J. J. G.; Moura, I. *J. Am. Chem. Soc.* **1999**, *121*, 2625−2626.
(13) Ljungdahl, L. G.; Andreesen, J. R. *FEBS Lett.* **1975**, *54*, 279−282.
(14) Yamamoto, I.; Saiki, T.; Liu, S.-M.; Ljungdahl, L. G. *J. Biol. Chem.* **1983**, *258*, 1826−1832.

10.1021/ic062441a CCC: $37.00
Published on Web 04/14/2007

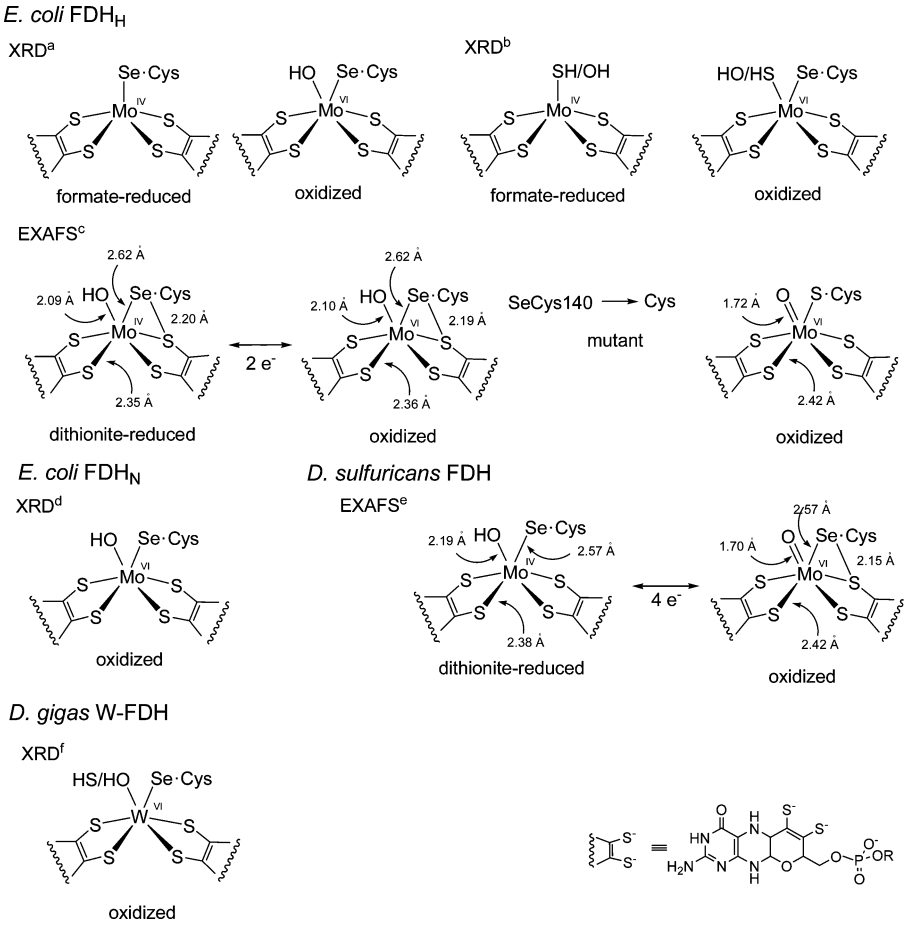

Figure 1. Schematic depictions of the active sites of FDHs obtained from X-ray diffraction or EXAFS analysis. Selected bond distances are indicated. In the pyranopterindithiolene structure, R is a nucleotide. References: [a]ref 7, [b]ref 8, [c]ref 11, [d]ref 9, [e]ref 12, [f]ref 10.

site structures, there are three features of note. (i) The metal atom is coordinated by *two* pyranopterindithiolene cofactor ligands, a defining feature of the DMSOR family of molybdenum enzymes. However, not all W−FDHs reported have been shown to contain two such ligands. (ii) Sites accommodate molybdenum and/or tungsten. Indeed, one organism (*Desulfovibrio alaskensis*) produces active Mo−FDH *and* W−FDH isoenzymes.[18] (iii) Selenocysteinate is coordinated in the oxidized and reduced states, with one possible exception[8] (Figure 1).

A necessary step prior to the development of analogue reaction systems is the synthesis of appropriate representations of the enzyme active sites. For nearly all native tungstoenzymes, the full coordination unit in any oxidation state has not been experimentally established. Molybdoenzyme members of the DMSOR family manifest terminal binding of endogenous serinate, cysteinate, or selenocysteinate and exogenous hydroxide/water and probably sulfide/hydrosulfide. Consequently, we have prepared and structurally characterized extensive sets of five-coordinate (L′ absent) and six-coordinate molybdenum and tungsten complexes $[MLL'(S_2C_2R_2)_2]^z$ containing variously substituted alkoxide, phenolate, and thiolate ligands as well as other ligand types. With M = W^{IV-VI}, ca. 25 complexes containing different ligand sets L and L,L′ have been prepared in this laboratory[1,20−22] and by others.[23−25] During the course of that work, we found selenolate complexes related to FDH sites difficult to prepare. The only known examples of such complexes are of the types $[Mo^{IV}(SeR)(S_2C_2Me_2)_2]^-$,[26] $[M^{IV}(CO)(SeR)(S_2C_2Me_2)_2]^-$ (M = Mo, W),[27,28] and $[W^{V}(SeR)_2(S_2C_2Me_2)_2]^-$.[29] Consequently, the present investigation was

(15) de Bok, F. A. M.; Hagedoorn, P.-L.; Silva, P. J.; Hagen, W. R.; Schlitz, E.; Fritsche, K.; Stams, A. J. M. *Eur. J. Biochem.* **2003**, *270*, 2476−2485.
(16) Laukel, M.; Christoserdova, L.; Lidstrom, M. E.; Vorholt, J. A. *Eur. J. Biochem.* **2003**, *270*, 325−333.
(17) Graentzdoerffer, A.; Rauh, D.; Pich, A.; Andreesen, J. R. *Arch. Microbiol.* **2003**, *179*, 116−130.
(18) Brondino, C. D.; Passeggi, M. C. G.; Caldeira, J.; Almendra, M. J.; Feio, M. J.; Moura, J. J. G.; Moura, I. *J. Biol. Inorg. Chem.* **2004**, *9*, 145−151.
(19) Rauh, D.; Graentzdoerffer, A.; Granderath, K.; Andreesen, J. R.; Pich, A. *Eur. J. Biochem.* **2004**, *271*, 212−219.
(20) Jiang, J.; Holm, R. H. *Inorg. Chem.* **2004**, *43*, 1302−1310.
(21) Wang, J.-J.; Kryatova, O.; Rybak-Akimova, E. V.; Holm, R. H. *Inorg. Chem.* **2004**, *43*, 8092−8101.
(22) Wang, J.-J.; Tessier, C.; Holm, R. H. *Inorg. Chem.* **2006**, *45*, 2979−2988.
(23) Ueyama, N.; Oku, H.; Nakamura, A. *J. Am. Chem. Soc.* **1992**, *114*, 7310−7311.
(24) Das, S. K.; Biswas, D.; Maiti, R.; Sarkar, S. *J. Am. Chem. Soc.* **1996**, *118*, 1387−1397.
(25) Oku, H.; Ueyama, N.; Nakamura, A. *Bull. Chem. Soc. Jpn.* **1996**, *69*, 3139−3150.
(26) Lim, B. S.; Holm, R. H. *J. Am. Chem. Soc.* **2001**, *123*, 1920−1930.
(27) Sung, K.-M.; Holm, R. H. *Inorg. Chem.* **2000**, *39*, 1275−1281.
(28) Lim, B. S.; Donahue, J. P.; Holm, R. H. *Inorg. Chem.* **2000**, *39*, 263−273.
(29) Sung, K.-M.; Holm, R. H. *Inorg. Chem.* **2001**, *40*, 4518−4525.

undertaken to develop synthetic routes to mononuclear bis(dithiolene)tungsten(IV,VI) selenolate complexes and to determine their structures. We have concentrated on tungsten rather than molybdenum in response to the existence of W−FDHs (albeit less well-defined than Mo−FDHs) and because of the instability of Mo^{VI} complexes containing dimethyldithiolene ligands to autoreduction to Mo^{V}.[26] As noted in previous reports, this dialkyldithiolene ligand provides an accurate simulation of the geometrical and electronic structural features of the native pyranopterindithiolene ligand cofactor (Figure 1).

Experimental Section

Preparation of Compounds. All reactions and manipulations were performed under anaerobic conditions using an inert atmosphere box and standard Schlenk techniques. Acetonitrile and ether were freshly purified using an Innovative Technology solvent purification system. Methanol was distilled from magnesium and THF, and hexanes were distilled from sodium benzophenone ketyl. Adamantane-1-thiol was a commercial sample (Aldrich). All solvent removal and drying steps were performed in vacuo. ^{1}H NMR data of salts refer to anions only. Compounds were identified by a combination of their mass spectra (in which parent ions were observed), ^{1}H NMR spectra, and X-ray crystal structures. Several representative compounds were subjected to elemental analysis.

2-Adamantylselenotrimethylsilane. A solution of 220 mg (0.51 mmol) of bis(2-adamantyl)diselenide[26] in 10 mL of THF was treated with 1.0 mL of a 1.0 M solution of $LiEt_3BH$ (2 equiv) in THF. The reaction mixture changed from yellow to milky white with vigorous gas evolution and was stirred for 2 h. Me_3SiCl (0.13 mL, 1.0 mmol) was added, the mixture was stirred overnight and filtered, and volatiles were removed from the filtrate. The remaining yellow liquid was extracted with hexanes, the solution was filtered, and hexane was evaporated to give the product as 118 mg (41%) of a bright-yellow oil. ^{1}H NMR ($CDCl_3$): δ 0.35 (s, 9), 1.54 (d, 2), 1.79 (m, 10), 2.22 (d, 2), 3.45 (s, 1).

1-Adamantylselenotrimethylsilane. The preceding method was used with bis(1-adamantyl)diselenide,[30,31] which was prepared by the procedure for the 2-adamantyl compound. ^{1}H NMR ($CDCl_3$): δ 0.44 (s, 9), 1.71 (m, 6), 2.00 (br s, 3), 2.17 (m, 6).

***tert*-Butylthiotrimethylsilane.** A mixture of 3.0 mL (0.027 mol) of Bu^tSH and 1.5 g (0.022 mol) of NaOEt in anhydrous methanol was stirred for 2 h, and the solvent was removed. The residue was suspended in acetonitrile, and 3.2 g (0.019 mol) of Et_4NCl was added. The mixture was stirred for 36 h and filtered, and the solvent was removed from the filtrate. The oily residue was dried for 2 h, leaving $(Et_4N)(SBu^t)$ as an off-white solid. This material (0.67 g, 3.1 mmol) was suspended in hexanes, and 0.33 g (3.0 mmol) of Me_3SiCl was added. The mixture was stirred for 5 h and filtered, and the solvent was removed to give the product as a clear liquid. ^{1}H NMR ($CDCl_3$): δ 0.35 (s, 9), 1.45 (s, 9). This compound was prepared earlier by a different method.[32]

tert*-Butylselenotrimethylsilane.** To an ethereal solution of Bu^t-MgCl (3.0 mmol) was added 236 mg (3.0 mmol) of gray selenium. As the mixture was stirred, the gray color gradually disappeared and a milky-white precipitate developed in 1−2 h. After 7 h, 0.50 g (3.0 mmol) of Me_3SiCl was added, the mixture was stirred for 4 h and filtered, and the solvent was removed from the filtrate. The cloudy oil was dissolved in 10 mL of hexane, an insoluble material was removed by filtration, and the solvent was removed to afford the product as 180 mg (29%) of yellow oil. (Caution***: *malodorous*!) This compound was prepared earlier using Bu^tLi at 0 °C. The ^{1}H NMR spectrum was the same as that of a sample prepared by that method.[33]

Tungsten(IV) Complexes. $(Et_4N)[W(SBu^t)(S_2C_2Me_2)_2]$. Method 1. To a solution of 95 mg (0.15 mmol) of $(Et_4N)[W(O_2CBu^t)(S_2C_2Me_2)_2]$[20] in 2 mL of acetonitrile was added a solution of 27 mg (0.17 mmol) of Me_3SiSBu^t in 0.5 mL of acetonitrile. The reaction mixture was stirred for 30 min, and the solvent was removed. The brown solid was washed with 10 mL of ether and dissolved in 3 mL of 2:1 (v/v) THF/acetonitrile, and the solution was layered with 20 mL of ether. The mixture was allowed to stand for 12 h. The pale-yellow solution was decanted, and the solid was washed with 5 mL of ether and dried, leading to 49 mg (53%) of product as a yellow crystalline solid. Absorption spectrum (acetonitrile): λ_{max} (ϵ_M) 311 (13 000), 343 (7000), 419 (4300), 501 (2400) nm. ES-MS: *m*/*z* 510 (M^-). ^{1}H NMR (CD_3CN): δ 0.97 (9), 2.81 (12). **Method 2.** A solution of 25 mg (0.052 mmol) of $[W(CO)_2(S_2C_2Me_2)_2]$[34] in 1 mL of THF was added with stirring to a solution of 11 mg (0.050 mmol) of $(Et_4N)(SBu^t)$ in 1 mL of acetonitrile. Vigorous gas evolution followed, and the mixture turned green. After 90 min, 20 mL of ether was layered on the mixture, which was allowed to stand for 12 h. The solid that separated was washed with ether and recrystallized from THF/acetonitrile/ether to give 20 mg (60%) of yellow crystals, spectroscopically identical to the product of method 1.

$(Et_4N)[W(S\text{-}1\text{-}Ad)(S_2C_2Me_2)_2]$. A solution of 97 mg (0.20 mmol) of $[W(CO)_2(S_2C_2Me_2)_2]$ in 2 mL of THF was mixed with a suspension of 39 mg (0.20 mmol) of NaS-1-Ad in 0.5 mL of acetonitrile. Upon stirring, the mixture formed a homogeneous green solution. After 30 min, 34 mg (0.20 mmol) of Et_4NCl in 0.5 mL of acetonitrile was added and stirring was continued for 5 h. The solvent was removed, and the orange-brown solid was washed with ether (6 mL) and dissolved in 3 mL of THF. Acetonitrile (1 mL) was added; the solution was covered with 20 mL of ether and allowed to stand for 20 h. The solid was collected, washed with ether, and dried, giving the product as 89 mg (61%) of orange crystalline solid. Absorption spectrum (acetonitrile): λ_{max} (ϵ_M) 310 (15 600), 343 (8200), 418 (4800), 502 (2650), 674 (650) nm. ES-MS: *m*/*z* 587 (M^-). ^{1}H NMR (CD_3CN): δ 1.42−1.52 (m, 12), 1.76 (br s, 3), 2.80 (12). Anal. Calcd for $C_{26}H_{47}NS_5W$: C, 43.50; H, 6.60; N, 1.95; S, 22.34. Found: C, 43.37; H, 6.52; N, 1.92; S, 21.38.

$(Et_4N)[W(SeBu^t)(S_2C_2Me_2)_2]$. To a solution of 102 mg (0.156 mmol) of $(Et_4N)[W(O_2CBu^t)(S_2C_2Me_2)_2]$ in 2 mL of acetonitrile was added 42 mg (0.20 mmol) of $Me_3SiSeBu^t$ in 0.5 mL of acetonitrile. After 2 min, formation of an orange solid was observed. The reaction mixture was stirred for 15 min, and the solvent was removed. The brown solid was washed with 6 mL of ether and dissolved in 3 mL of 2:1 (v/v) THF/acetonitrile, and the solution was layered with 20 mL of ether. After 12 h, the solid that separated was collected, washed with 10 mL of ether, and dried to afford the product as 77 mg (72%) of a yellow-orange solid. Absorption spectrum (acetonitrile): λ_{max} (ϵ_M) 318 (15 400), 382 (sh, 5500), 424 (5200), 507 (3200) nm. ES-MS: *m*/*z* 557 (M^-). ^{1}H NMR (CD_3CN): δ 1.11 (9), 2.84 (12).

$(Et_4N)[W(Se\text{-}1\text{-}Ad)(S_2C_2Me_2)_2]$. To a solution of 113 mg (0.181 mmol) of $(Et_4N)[W(O_2CBu^t)(S_2C_2Me_2)_2]$ in 2 mL of acetonitrile

(30) Palacios, S. M.; Santiago, A. N.; Rossi, R. A. *J. Org. Chem.* **1984**, *49*, 4609−4613.
(31) Barton, D. H. R.; Fontana, G. *Tetrahedron* **1996**, *52*, 11163−11176.
(32) Kuwajima, I.; Abe, T. *Bull. Chem. Soc. Jpn.* **1978**, *51*, 2183−2184.
(33) Zhu, N.; Fenske, D. *J. Chem. Soc., Dalton Trans.* **1999**, 1067−1075.
(34) Goddard, C. A.; Holm, R. H. *Inorg. Chem.* **1999**, *38*, 5389−5398.

was added 73 mg (0.25 mmol) of Me_3SiSe-1-Ad. The color changed to red-orange. and a bright-orange solid precipitated. The reaction mixture was stirred for 10 min, and the solvent was removed. The solid residue was washed with ether (10 mL) and dissolved in THF/acetonitrile (2:1, v/v). The red-orange solution was filtered, and ether was layered on the filtrate. After 2 h, the pale-brown solution was decanted and the remaining solid was washed with ether (6 mL) and dried to afford the product as 100 mg (72%) of orange needlelike crystals. Absorption spectrum (acetonitrile): λ_{max} (ϵ_M) 318 (18 900), 381 (sh, 5800), 424 (4900), 507 (2400). ES-MS: *m*/*z* 635 (M^-). ^1H NMR (CD_3CN): δ 1.50 (m, 6), 1.65 (m, 6), 1.76 (br s, 3), 2.83 (12).

(Et_4N)[W(Se-2-Ad)($S_2C_2Me_2$)$_2$]. To a solution of 47 mg (0.072 mmol) of (Et_4N)[W(O_2CBu^t)($S_2C_2Me_2$)$_2$] in 1 mL of acetonitrile was added a solution of 31 mg (0.11 equiv) of Me_3SiSe-2-Ad in 0.5 mL of acetonitrile. Within 2 min, an orange solid appeared. The reaction mixture was stirred for 3 min, and the solvent was removed. The red-orange solid was washed with 10 mL of ether and dissolved in 3 mL of 2:1 (v/v) THF/acetonitrile. The solution was filtered, and ether was layered on the filtrate. After 3 h, the brown solution was decanted; the solid was washed with 6 mL of ether and dried to afford the product as 36 mg (65%) of red-orange needles. Absorption spectrum (acetonitrile): λ_{max} (ϵ_M) 317 (15 200), 374 (sh, 5600), 425 (4300), 500 (1200) nm. ES-MS: *m*/*z* 635 (M^-). ^1H NMR (CD_3CN): δ 1.35 (d, 2), 1.47 (d, 2), 1.61 (br s, 3), 1.70 (m, 2), 1.73 (br s, 3), 1.80 (d, 2), 2.85 (s, 12), 3.27 (s, 1). Anal. Calcd for $C_{26}H_{47}NS_4SeW$: C, 40.84; H, 6.19; N, 1.83. Found: C, 40.57; H, 6.37; N, 1.66.

(Et_4N)[W(CO)($SeBu^t$)($S_2C_2Me_2$)$_2$]. To a solution of 50 mg (0.11 mmol) of [W(CO)$_2$($S_2C_2Me_2$)$_2$] in 2 mL of THF was added a solution of 33 mg (0.13 mmol) of (Et_4N)($SeBu^t$) in 0.5 mL of acetonitrile. Vigorous gas evolution occurred immediately, and the reaction mixture became green. The mixture was stirred for 35 min, and the solvent was removed. The solid was washed with 6 mL of ether and dissolved in THF (ca. 3 mL), and the solution was covered with 20 mL of ether. After 24 h, the solid that separated was collected, washed with ether, and dried to give the product as 49 mg (65%) of a green microcrystalline solid. Absorption spectrum (acetonitrile): λ_{max} (ϵ_M) 365 (5200), 424 (4500), 602 (3900) nm. IR (KBr): ν_{CO} 1921 cm^{-1}. ES-MS: *m*/*z* 585 (M^-). ^1H NMR (CD_3CN): δ 1.65 (9), 2.48 (12).

(Et_4N)[W(CO)(Se-1-Ad)($S_2C_2Me_2$)$_2$]. To a bright-yellow solution of 35 mg (0.082 mmol) of bis(1-adamantyl)diselenide in 1 mL of THF was added 0.13 mL of (0.13 mmol) of a 1.0 M solution of $LiEt_3BH$ in THF. The yellow color disappeared as gas evolution occurred. This solution was added in one portion to a solution of 62 mg (0.13 mmol) of [W(CO)$_2$($S_2C_2Me_2$)$_2$]. Vigorous gas evolution occurred immediately, and the reaction mixture became green. After 30 min, a solution of 21 mg (0.13 mmol) of Et_4NCl in 1 mL of acetonitrile was added, the mixture was stirred for 10 min, and the solvent was removed. The greenish-brown solid residue was washed with ether and dissolved in ca. 3 mL of THF, and 20 mL of ether was layered on the solution. Two crops of solid were isolated, affording the product as 28 mg (27%) of green crystals. Absorption spectrum (acetonitrile): λ_{max} (ϵ_M) 276 (sh, 9200), 317 (sh, 6560), 437 (5200), 616 (2600) nm. IR (KBr): ν_{CO} 1919 cm^{-1}. ES-MS: *m*/*z* 663 (M^-), 635 ({M−CO}$^-$). NMR (CD_3CN): δ 1.75 (m, 6), 1.96 (br s, 3), 2.26 (br s, 6), 2.48 (12).

Tungsten(VI) Complexes. (Et_4N)[WO(SBu^t)($S_2C_2Me_2$)$_2$]. A solution of 83 mg (0.13 mol) of (Et_4N)[W(SBu^t)($S_2C_2Me_2$)$_2$] in 1 mL of acetonitrile was treated with a solution of 50 mg (0.16 mmol) of Ph_3AsO in 2 mL of THF. A slow color change to intense purple occurred over 5 min. The reaction mixture was stirred for 30 min, 20 mL of cold ether was added, and the mixture was allowed to stand at −30 °C for 1 day. The pale-purple solution was decanted from a purple solid, which was washed with cold ether (2 × 3 mL) and dried. The product was obtained as 79 mg (93%) of purple solid. Absorption spectrum (acetonitrile): λ_{max} (ϵ_M) 298 (sh, 8200), 406 (3750), 557 (3500), 686 (sh, 1650) nm. ES-MS: *m*/*z* 525 (M^-). ^1H NMR (CD_3CN): δ 1.46 (9), 2.19 (12).

(Et_4N)[WO(S-1-Ad)($S_2C_2Me_2$)$_2$]. To a solution of 89 mg (0.12 mmol) of (Et_4N)[W(S-1-Ad)($S_2C_2Me_2$)$_2$] in 1 mL of acetonitrile was added in one portion a solution of 47 mg (0.15 mmol) of Ph_3AsO in 1 mL of THF. A color change to intense purple was observed within 5 min. The reaction mixture was stirred for 30 min. Cold ether (30 mL) was added, and the mixture was allowed to stand at −30 °C for 1 day. The pale-purple solution was decanted, and the solid residue was washed with cold ether (2 × 3 mL) and dried to afford the product as 76 mg (84%) of a purple solid. Absorption spectrum (acetonitrile): λ_{max} (ϵ_M) 300 (sh, 8900), 421 (3750), 559 (4500), 689 (sh, 1900) nm. ES-MS: *m*/*z* 603 (M^-). ^1H NMR (CD_3CN): δ 1.64 (m, 6), 1.95 (br s, 3), 2.06 (m, 6), 2.18 (12).

(Et_4N)[WO($SeBu^t$)($S_2C_2Me_2$)$_2$]. To a solution of 38 mg (0.055 mmol) of (Et_4N)[W($SeBu^t$)($S_2C_2Me_2$)$_2$] in 2 mL of acetonitrile was added a solution of 22 mg (0.068 mmol) of Ph_3AsO in 2 mL of THF, resulting in a slow color change to brown. After 3 min, 20 mL of cold ether was added and the solution was allowed to stand at −30 °C. After 3 h, the blue solution was separated from a brown solid and maintained at −30 °C for 3 h. The blue microcrystalline solid that separated was isolated, washed with 2 × 3 mL of cold ether, and dried, affording 18 mg (47%) of product. Absorption spectrum (acetonitrile): λ_{max} (ϵ_M) 304 (sh, 5800), 429 (2400), 581 (2950), 697 (sh, 1800) nm. ES-MS: 573 (M^-). ^1H NMR (CD_3CN): δ 1.59 (9), 2.19 (12).

(Et_4N)[WO(Se-1-Ad)($S_2C_2Me_2$)$_2$]. A solution of 46 mg (0.060 mmol) of (Et_4N)[W(Se-1-Ad)($S_2C_2Me_2$)$_2$] in 1 mL of acetonitrile was treated with a solution of 23 mg (0.072 mmol) of Ph_3AsO in 1 mL of THF in one portion. A color change to blue was observed within 1−2 min. The reaction mixture was stirred for 7 min, and 20 mL of cold ether was layered on the solution. The mixture was left to stand at −30 °C for 1 day. The pale-blue solution was decanted. The solid residue was washed with cold ether and dried to yield the product as 25 mg (53%) of a gray-blue solid. Absorption spectrum (acetonitrile): λ_{max} (ϵ_M) 299 (sh, 9200), 437 (sh, 3000), 587 (3200), 689 (sh, 2500) nm. ES-MS: *m*/*z* 651 (M^-). ^1H NMR (CD_3CN): δ 1.67 (m, 6), 1.95 (br s, 3), 2.18 (12), 2.20 (m, 6).

(Et_4N)[WS(S-1-Ad)($S_2C_2Me_2$)$_2$]. A solution of 30 mg (0.042 mmol) of (Et_4N)[W(S-1-Ad)($S_2C_2Me_2$)$_2$] in 1 mL of acetonitrile was cooled to −30 °C. A solution of 16 mg (0.041 mmol) of Ph_3SbS in 1 mL of THF at −30 °C was added in one portion with stirring. A color change from orange-brown to purple was observed within seconds. The reaction mixture was stirred for 2 min, 20 mL of cold ether was added, and the mixture was allowed to stand at −30 °C overnight. The solid that separated was washed with cold ether and dried to give the product as 28 mg (89%) of a dark-violet solid. Absorption spectrum (acetonitrile): λ_{max} (ϵ_M) 333 (9100), 374 (7500), 556 (6100) nm. ES-MS: *m*/*z* 619 (M^-). ^1H NMR (CD_3CN): δ 1.64 (br s, 6), 2.00 (br s, 9), 2.30 (s, 12). Anal. Calcd. for $C_{26}H_{47}NS_6W$: C, 41.64; H, 6.32; N, 1.87. Found: C, 41.54; H, 6.30; N, 1.90.

(Et_4N)[WS(Se-1-Ad)($S_2C_2Me_2$)$_2$]. The preceding method was used based on 43 mg (0.056 mmol) of (Et_4N)[W(Se-1-Ad)($S_2C_2Me_2$)$_2$]. A rapid color change to purple-blue occurred. The dark-purple solid that separated in ca. 1 h after the addition of ether was discarded, and the remaining blue-gray solution was cooled to −30

°C. After 3 h, the pale-blue solution was decanted and the solid that separated was washed with cold ether and dried. The product was obtained as 19 mg (43%) of a gray-blue solid. Absorption spectrum (acetonitrile): λ_{max} (ϵ_M) 333 (8000), 383 (sh, 5500), 573 (5200) nm. ES-MS: *m*/*z* 667 (M^-). ^{1}H NMR (CD_3CN): δ 1.69 (br s, 6), 1.95 (br s, 3), 2.13 (br s, 6), 2.30 (s, 12).

[W(SBu^t)(OSiMe$_3$)(S$_2$C$_2$Me$_2$)$_2$]. To a stirred suspension of 65 mg (0.100 mmol) of (Et_4N)[WO(SBu^t)($S_2C_2Me_2$)$_2$] in 2 mL of toluene was added 0.24 mL (0.094 mmol) of a 0.39 M solution of Me_3SiCl in toluene. The reaction mixture was stirred for 1 h and filtered, and the solvent was removed. The brown solid was extracted with a minimal volume of hexane, the solution was filtered, and the solvent was removed from the filtrate, leaving the product as 20 mg (33%) of a brown solid. Absorption spectrum (hexane): λ_{max} (ϵ_M) 302 (4650), 378 (4400), 487 (3500), 585 (2750) nm. ES-MS: *m*/*z* 598.0 (M^-). ^{1}H NMR (C_6D_6): δ 0.36 (9), 1.45 (9), 2.35 (12). Over several days in solution (ether, hexane), the complex partially decomposes, forming [W($S_2C_2Me_2$)$_3$] (identified by ^{1}H NMR[7]).

[W(SC$_6$H$_2$-2,4,6-Pr$^i_3$)(OSiMe$_3$)(S$_2$C$_2$Me$_2$)$_2$]. To a stirred suspension of 79 mg (0.098 mmol) of purple (Et_4N)[WO(SC$_6$H$_2$-2,4,6-Pr$^i_3$)($S_2C_2Me_2$)$_2$][20] in 2 mL of toluene was added 0.22 mL of a 0.39 M solution of Me_3SiCl (0.90 equiv) in toluene. The reaction mixture was stirred for 40 min as the color gradually changed to brown and was filtered, and the solvent was removed from the filtrate. The red-brown solid contained the desired product and ca. 8% [W($S_2C_2Me_2$)$_3$] (^{1}H NMR). The latter was removed by extraction with a minimal volume of hexane, leaving the product as 30 mg (45%) of a red-brown solid. Absorption spectrum (hexane): λ_{max} (ϵ_M) 282 (sh, 7000), 391 (8150), 525 (sh, 4300), 600 (2900) nm. ES-MS: *m*/*z* 745 (M^-). ^{1}H NMR (C_6D_6): δ 1.18 (d, 6), 1.32 (d,-12), 2.38 (s, 12), 2.76 (sept, 1), 3.95 (sept, 2), 6.97 (s, 2).

[W(SC$_6$H$_2$-2,4,6-Pr$^i_3$)$_2$(S$_2$C$_2$Me$_2$)$_2$]. This compound was isolated in small yield as a reaction byproduct and was identified by an X-ray structure determination. To a stirred suspension of 44 mg (0.054 mmol) of (Et_4N)[WO(SC$_6$H$_2$-2,4,6-Pr$^i_3$)($S_2C_2Me_2$)$_2$] in 2 mL of THF was added 0.07 mL of a 0.39 M solution of Me_3SiCl (0.027 mmol). The reaction mixture immediately turned to red-brown, was stirred for 45 min and filtered, and the solvent was removed from the filtrate to give a brown solid. The solid was dissolved in ether and maintained at −30 °C. After several days, brown crystals were separated, washed with cold ether, and dissolved in hexanes. The solution was filtered, and the solvent was removed from the filtrate to given a brown solid, which was dried to give ∼4 mg of product. ES-MS: *m*/*z* 745 (M^-). ^{1}H NMR (C_6D_6): δ 1.23 (d, 12), 1.35 (br s, 24), 2.32 (s, 12), 2.80 (2), ∼3.5 (v br, 4), 6.95 (br, 4).

[W(S-1-Ad)(OSiMe$_3$)(S$_2$C$_2$Me$_2$)$_2$]. To a stirred suspension of 25 mg (0.034 mmol) of purple (Et_4N)[WO(S-1-Ad)($S_2C_2Me_2$)$_2$] in 2 mL of toluene was added 0.09 mL (0.035 mmol) of a 0.39 M solution of Me_3SiCl in toluene. The reaction mixture, which slowly assumed a red-brown color, was stirred for 1 h and filtered, and the solvent was removed from the filtrate to give a brown solid. The solid was extracted with hexane. Solvent was removed from the solution to yield the product as 12 mg (52%) of a red-brown solid. Absorption spectrum (hexanes): λ_{max} (ϵ_M) 282 (sh, 9700), 383 (7300), 441 (6000), 488 (sh, 5800), 579 (sh, 2900) nm. ES-MS: *m*/*z* 676 (M^-). ^{1}H NMR (C_6D_6): δ 0.37 (s, 9), 1.45 (m, 6), 1.87 (br s, 3), 2.12 (s, 12), 2.33 (s, 12).

[W(S-1-Ad)(OSiPh$_3$)(S$_2$C$_2$Me$_2$)$_2$]. To a stirred suspension of 54 mg (0.074 mmol) of (Et_4N)[WO(S-1-Ad)($S_2C_2Me_2$)$_2$] in 2 mL of toluene was added a solution of 20 mg (0.066 mmol) of Ph_3SiCl in 1 mL of toluene. The reaction mixture immediately turned red and was stirred for 15 min, during which the red color became more intense and more solid dissolved. The mixture was filtered, and the solvent was removed from the filtrate, leaving a red-brown solid. This material was washed with hexanes and ether and dried to give the product as 22 mg (39%) of a dark-red solid. Absorption spectrum (toluene): λ_{max} (ϵ_M) 386 (8100), 491 (6500), 579 (sh, 4500) nm. ^{1}H NMR (C_6D_6): δ 1.38 (br, 6), 1.80 (br, 3), 1.92 (m, 6), 2.31 (12), 7.19 (m, H), 7.97 (m, 6).

Tungsten(V) Complexes. (Et$_4$N)$_2$[W$_2$(μ_2-S)$_2$(S$_2$C$_2$Me$_2$)$_4$]. A solution of 25 mg (0.052 mmol) of [W(CO)$_2$($S_2C_2Me_2$)$_2$] in 1 mL of THF was added with stirring to a solution of 11 mg (0.050 mmol) of (Et_4N)(SBu^t) in 1 mL of acetonitrile. The mixture turned green with vigorous gas evolution and was stirred overnight, during which it assumed an orange-brown color. An ^{1}H NMR spectrum of a solid obtained from the reaction mixture indicated a ∼3:1 mixture of [W(SBu^t)($S_2C_2Me_2$)$_2$]$^-$ and the product. The reaction mixture was stirred for 3 days, layered with 20 mL of ether, and allowed to stand overnight. The precipitate was collected, washed with ether, and dried to afford the product as 12 mg (41%) of a purple solid. Absorption spectrum (acetonitrile): λ_{max} (ϵ_M) 267 (25 600), 336 (13 900), 404 (11 400), 492 (10 500), 560 (sh, 8800) nm. ES-MS: *m*/*z* 1036.5 ({(Et_4N)[W_2S_2($S_2C_2Me_2$)$_4$]}$^-$), 452 ([WS($S_2C_2Me_2$)$_2$]$^-$). ^{1}H NMR (CD_3CN): δ 2.26. This compound has also been prepared by other methods.[29]

(Et$_4$N)$_2$[W$_2$(μ_2-Se)$_2$(S$_2$C$_2$Me$_2$)$_4$]. A solution of 17 mg (0.026 mmol) of (Et_4N)[W(SeBu^t)($S_2C_2Me_2$)$_2$] in 2 mL of acetonitrile was stirred for 20 h, during which the color slowly changed from red-orange to brown-black. The solvent was removed, and the solid residue was recrystallized from acetonitrile/ether to afford the product as 13 mg (77%) of a purple-black solid. Absorption spectrum (acetonitrile): λ_{max} (ϵ_M) 271 (26 300), 351 (14 200), 409 (13 100), 440 (14 500), 529 (12 000) nm. ES-MS: *m*/*z* 1128 ({(Et_4N)[W_2Se_2($S_2C_2Me_2$)$_4$]}$^-$), 500.3 ([WSe($S_2C_2Me_2$)$_2$]$^-$). ^{1}H NMR (CD_3CN): δ 2.31.

(Et$_4$N)$_2$[MoS(S$_2$C$_2$Me$_2$)$_2$]. A dark-violet solution of 50 mg (0.13 mmol) of [Mo(CO)$_2$($S_2C_2Me_2$)$_2$][28] in 2 mL of THF was added in one portion to a solution of 42 mg (0.26 mmol) of (Et_4N)(SH) in 1 mL of acetonitrile. A color change to green and gas evolution were observed. The reaction mixture was stirred for 1 h, the solvent was removed, and the residue was dissolved in 2 mL of acetonitrile. The solution was covered with THF. The solid that separated after 1 day was washed with THF and dried to give the product as 60 mg (74%) of a microcrystalline green-brown solid. Absorption spectrum (acetonitrile): λ_{max} (ϵ_M) 268 (16 200), 310 (10 000), 398 (4600), 462 (2000) nm. ES-MS: *m*/*z* 626 ({(Et_4N)$_2$[MoS($S_2C_2Me_2$)$_2$]}$^+$). ^{1}H NMR (CD_3CN): δ 2.36 (br). Anal. Calcd for $C_{24}H_{52}MoN_2S_5$: C, 46.12; H, 8.39; N, 4.48; S, 25.65. Found: C, 45.91; H, 8.12; N, 4.36; S, 24.66. $E_{1/2}$ = −0.65 V (2−/1−, acetonitrile).

X-ray Structure Determinations. The structures of the 14 compounds in Tables 1 and 2 were determined. For simplicity, the compounds are referred to by the numerical designations of their complexes in Table 3. Diffraction-quality crystals of **3**−**7** were obtained by layering ether onto concentrated acetonitrile/THF solutions and allowing the mixtures to stand overnight. Crystals of **10**−**12** were grown similarly but with mixtures maintained at −30 °C for longer periods. Crystals of **19** were obtained by slow concentration of a toluene solution, and those of **20** were obtained from a saturated ether solution at −30 °C. Crystals of **21** formed upon ether diffusion into an acetonitrile solution at room temperature, and those of **22** and **23** were grown in a similar manner from solutions at −30 °C.

Crystals were coated in grease and mounted on a Siemens (Bruker) SMART CCD instrument using Mo Kα radiation. Data were collected at 193 K with scans of 0.3°/frame for 10, 20, or 30

Table 1. Crystallographic Data and Structure Refinement Parameters for **3**−**7**, **10**, and **11**

	(Et_4N)[**3**]	(Et_4N)[**4**]	(Et_4N)[**5**]	(Et_4N)[**6**]	(Et_4N)[**7**]	(Et_4N)[**10**]	(Et_4N)[**11**]·CH_3CN
formula	$C_{20}H_{41}NS_5W$	$C_{26}H_{47}NS_5W$	$C_{20}H_{41}NS_4SeW$	$C_{26}H_{47}NS_4SeW$	$C_{26}H_{47}NS_4SeW$	$C_{20}H_{41}NOS_5W$	$C_{26}H_{44}NOS_5W$
fw	639.69	717.80	686.59	764.70	764.70	655.69	793.86
cryst syst	monoclinic	monoclinic	monoclinic	tetragonal	tetragonal	monoclinic	triclinic
space group	$P2_1/n$	$P2_1/n$	$P2_1/n$	$I4_1/a$	$I4_1/a$	$P2_1/n$	$P\bar{1}$
Z	4	4	4	16	16	4	2
a, Å	10.888(1)	10.894(1)	10.895(3)	36.01(2)	36.315(3)	9.504(1)	11.011(1)
b, Å	21.931(2)	24.802(1)	22.103(6)	36.02(1)	36.315(3)	16.525(2)	11.819(1)
c, Å	11.311(1)	11.476(1)	11.330(3)	9.885(8)	9.736(2)	17.415(3)	14.844(1)
α, deg	90	90	90	90	90	90	74.006(1)
β, deg	97.963(1)	96.536(1)	98.595(6)	90	90	103.404(3)	88.728(1)
γ, deg	90	90	90	90	90	90	70.253(1)
V, Å^3	2674.7(4)	3080.5(3)	2697.9(13)	12816(15)	12839(3)	2660.4(7)	1742.5(2)
d_{calcd}, g/cm^3	1.589	1.548	1.690	1.585	1.582	1.637	1.513
μ, mm^{-1}	4.716	4.104	5.947	5.017	5.008	4.746	3.639
2θ range, deg	3.8−56.6	3.2−55.8	3.6−50.0	2.2−55.9	2.2−56.7	3.4−55.8	3.8−55.9
R1[a] (wR2[b]), %	4.63 (10.41)	3.79 (7.52)	7.82 (14.11)	4.64 (11.41)	3.99 (10.25)	5.95 (9.22)	3.80 (8.64)
GOF (F^2)	1.111	1.057	0.992	1.118	1.025	0.994	1.109

[a] $R1 = \sum||F_o| - |F_c||/\sum|F_o|$. [b] $wR2 = \{\sum[w(F_o^2 - F_c^2)^2/\sum(F_o^2)^2]\}^{1/2}$.

Table 2. Crystallographic Data and Structure Refinement Parameters for **12** and **19**−**24**

	(Et_4N)[**12**]	**19**	**20**	$(Et_4N)_2$[**21**]·CH_3CN	$(Et_4N)_2$[**22**]·CH_3CN	$(Et_4N)_2$[**23**]·$6CH_3CN$	(Et_4N)[**24**]
formula	$C_{20}H_{41}NOS_4SeW$	$C_{36}H_{42}OS_5SiW$	$C_{38}H_{58}S_6W$	$C_{26}H_{55}MoN_3S_5$	$C_{36}H_{70}N_4S_{10}W_2$	$C_{44}H_{82}N_8S_8Se_2W_2$	$C_{24}H_{44}NS_8SeW_2$
fw	702.59	862.94	891.05	665.97	1247.26	1505.28	1049.74
cryst syst	monoclinic	monoclinic	triclinic	triclinic	monoclinic	triclinic	monoclinic
space group	$P2_1/n$	$P2_1/c$	$P\bar{1}$	$P\bar{1}$	$P2_1/n$	$P1$	$P2_1/c$
Z	4	4	2	4	2	1	4
a, Å	9.521(1)	10.945(2)	10.546(2)	13.201(1)	11.300(1)	10.971(2)	10.035(2)
b, Å	16.522(2)	12.904(2)	14.131(2)	13.747(1)	15.347 (2)	11.675(1)	16.524(3)
c, Å	17.570 (2)	25.552(4)	14.663(3)	19.267(1)	14.930(2)	13.732(2)	20.663(4)
α, deg	90	90	96.490(4)	95.866(1)	90	69.463(2)	90
β, deg	103.435(2)	91.022(3)	94.872(3)	94.090(1)	107.755(2)	68.356(2)	95.856(4)
γ, deg	90	90	102.656(3)	90.356(1)	90	70.839(2)	90
V, Å^3	2688.2(5)	3608.1(9)	2104.8(6)	3468.9(4)	2466.0(5)	1490.5(3)	3408(1)
d_{calcd}, g/cm^3	1.736	1.589	1.406	1.275	1.680	1.677	2.046
μ, mm^{-1}	5.974	3.552	3.066	0.698	5.114	5.394	8.320
2θ range, deg	3.4−55.9	3.2−56.0	2.8−50.0	2.1−55.9	2.9−55.8	2.8−55.9	4.7−55.8
R1[a] (wR2[b]), %	5.29 (9.97)	3.93 (9.37)	5.92 (14.3)	6.30 (11.63)	5.49 (10.23)	2.65 (7.00)	3.99 (7.14)
GOF (F^2)	0.978	1.042	1.014	0.954	1.298	1.038	1.018

[a] $R1 = \sum||F_o| - |F_c||/\sum|F_o|$. [b] $wR2 = \{\sum[w(F_o^2 - F_c^2)^2/\sum(F_o^2)^2]\}^{1/2}$.

s frames, such that 1271 frames were collected for a hemisphere of data. The first 50 frames were recollected at the end of the data collection to monitor intensity decay; no significant decay was observed from any compound. Data out to 2θ of 50° were used for **5** and **20** because of the somewhat lower quality of the high-angle data; for other compounds, data out to 2θ of 56° were employed. Cell parameters were retrieved using SMART software and refined with SAINT software on all observed reflections in the 2θ range. Data reduction was performed with SAINT, which corrects for Lorentz polarization and decay. All space groups were assigned by analysis of symmetry and systematic absences determined by XPREP. Structures were solved by direct methods and SHELXL-97 and refined against all data in the 2θ ranges by full-matrix least squares on F^2. All non-hydrogen atoms were refined anisotropically. Hydrogen atoms at idealized positions were included in the final refinements. The 1-Ad group of **4** was found in two overlapping conformations that could be accurately modeled. The cation in **7** and one of the isopropyl groups in **20** were disordered; the disorders were treated in terms of two conformations. The disorder of the 1-Ad group of **19** could not be resolved. Crystal parameters and agreement factors are reported in Tables 1 and 2.[35]

(35) See paragraph at the end of this article for Supporting Information available.

Other Physical Measurements. All measurements were performed under anaerobic conditions. ^{1}H NMR spectra were recorded with a Bruker DMX-500 or a Varian Mercury 300/400 spectrometer. Absorption spectra were obtained with a Varian Cary 50 Bio spectrophotometer, and infrared spectra were obtained with a Nicolet 5PC FT-IR instrument. Electrospray mass spectra were measured on acetonitrile solutions of salts or hexane solutions of neutral compounds directly infused into an LCT mass spectrometer. Cyclic voltammograms were recorded using a PAR model 263 potentiostat/galvanostat and a glassy-carbon working electrode, with 0.1 M $(Bu_4N)(PF_6)$ supporting electrolyte; potentials are referenced to the saturated calomel electrode.

Results and Discussion

The structural information in Figure 1 indicates that suitable FDH active site analogues require the preparation of reduced (M^{IV}) and oxidized (M^{VI}) bis(dithiolene) complexes with variant additional ligation that includes selenolate binding in all but one proposed case. Compiled in Table 3 are all previously known bis(dithiolene)molybdenum and -tungsten monoselenolate complexes and their thiolate counterparts and complexes **3**−**24** prepared in this investigation by the reactions in Schemes 1 and 2. No attempt has

Table 3. Synthetic Bis(dithiolene)molybdenum and -tungsten Complexes: Numerical Designations and Selected Examples Relevant to Proposed or Established Coordination Units in Formate Dehydrogenases

Mo^{IV}/W^{IV}	
$[Mo(SR)(S_2C_2Me_2)_2]^-$	R = 2-Ad,[a] C_6H_2-2,4,6-Pr^i_3[b]
$[W(SR)(S_2C_2Me_2)_2]^-$	R = Bu^t (**3**), 1-Ad (**4**), C_6H_2-2,4,6-Pr^i_3[c]
$[Mo(Se\text{-}2\text{-}Ad)(S_2C_2Me_2)_2]^-$ [a]	
$[W(SeR)(S_2C_2Me_2)_2]^-$	R = Bu^t (**5**), 1-Ad (**6**), 2-Ad (**7**)
$[Mo(CO)(SeR)(S_2C_2Me_2)_2]^-$	R = Ph, C_6H_2-2,4,6-Pr^t_3[b]
$[W(CO)(SeR)(S_2C_2Me_2)_2]^-$	R = Bu^t (**8**), 1-Ad (**9**), Ph, C_6H_2-2,4,6-Pr^i_3[d]
$[MoS(S_2C_2Me_2)_2]^{2-}$	**21**
$[WS(S_2C_2Me_2)_2]^{2-}$ [e]	
W^{VI}	
$[WO(SR)(S_2C_2Me_2)_2]^-$	R = Bu^t (**10**), 1-Ad (**11**), Ph, C_6H_2-2,4,6-Pr^i_3[d]
$[WO(SeR)(S_2C_2Me_2)_2]^-$	R = Bu^t (**12**), 1-Ad (**13**)
$[WS(SC_6H_2\text{-}2,4,6\text{-}Pr^i_3)(S_2C_2Me_2)_2]^-$ [c]	
$[WS(S\text{-}1\text{-}Ad)(S_2C_2Me_2)_2]^-$	**14**
$[WS(Se\text{-}1\text{-}Ad)(S_2C_2Me_2)_2]^-$	**15**
$[W(SR)(OSiMe_3)(S_2C_2Me_2)_2]^-$	R = Bu^t (**16**), C_6H_2-2,4,6-Pr^i_3 (**17**)
$[W(S\text{-}1\text{-}Ad)(OSiR_3)(S_2C_2Me_2)_2]$	R = Me (**18**), Ph (**19**)
$[W(SC_6H_2\text{-}2,4,6\text{-}Pr^i_3)_2(S_2C_2Me_2)_2]$	**20**
$W^{V,IV/V}$	
$[W_2(\mu_2\text{-}S)_2(S_2C_2Me_2)_4]^{2-}$	**22**
$[W_2(\mu_2\text{-}Se_2)_2(S_2C_2Me_2)_4]^2$	**23**
$[W_2(\mu_2\text{-}Se)(S_2C_2Me_2)_4]^-$	**24**

[a] Reference 26. [b] Reference 28. [c] Reference 20. [d] Reference 27. [e] Reference 29.

been made to prepare the highly unusual structures with interligand Se−S bonds deduced from EXAFS analysis of *Escherichia coli* FDH_H and *D. desulfuricans* FDH. Note the close structural and electronic relationship in the immediate coordination environment between the 1,2-dimethyldithiolene ligand and the chelating functionality of the pyranopterin-dithiolene cofactor ligand. In the following sections, syntheses are considered in terms of the tungsten oxidation state; all anionic complexes were isolated at Et_4N^+ salts in the indicated yields. Synthesis descriptions extend in some cases to identification of the decomposition products of isolated complexes and reaction byproducts. Structural descriptions are provided with the use of Figures 2−5 and Tables 4−6. Metric parameters are limited to selected bond distances and to angles that define the overall stereochemistry. Because they are nearly constant over the set of complexes, certain other parameters such as chelate bite angles (79−83°) and atom deviations from nearly planar chelate rings are omitted.[35] Chelate ring C−C and S−C bond lengths[35] fall in the intervals of 1.32−1.36 and 1.71−1.77 Å, respectively, with the large majority of values in the centers of the intervals. As with all prior $[ML(S_2C_2Me_2)_2]^-$ and $[MLL'(S_2C_2Me_2)_2]^-$ complexes, these values correspond to an enedithiolate(2−) ligand description. In the latter complexes, we use the transoid (interchelate) S−M−S angle as a shape parameter for (distorted) octahedral vs trigonal-prismatic stereochemistry.[36]

Tungsten(IV) Complexes. (a) Synthesis and Structures. Two approaches were employed utilizing as precursors the dicarbonyl $[W(CO)_2(S_2C_2Me_2)_2]$ (**1**)[34] and the carboxylate $[W(O_2CBu^t)(S_2C_2Me_2)_2]^-$ (**2**).[20] One is based on previous observations of the generalized reaction 1 (M = Mo, W; Q = O, S, Se). With M = Mo, all reactants RO^- and thiolates and selenolates with bulky substituents (R = 2,4,6-$Pr^i_3C_6H_2$, 2-Ad) lead to complete carbonyl substitution ($n = 2$)

$$[M(CO)_2(S_2C_2Me_2)_2] + RQ^- \rightarrow [M(CO)_{2-n}(QR)(S_2C_2Me_2)_2]^- + nCO \quad (1)$$

whereas PhS^- and $PhSe^-$ afford monocarbonyl products ($n = 1$).[26,28] With M = W, the principal difference is that monocarbonyls are formed with the same large thiolate and selenolate reactants. These results have been rationalized on the basis of the bond length order M−OR < M−SR < M−SeR, leading to decreasing steric interaction between the carbonyl and R substituent, and the bond strength order Mo−CO < W−CO. In this work, we have employed the sterically demanding groups R = Bu^t and 1-Ad in an attempt to disrupt carbonyl binding and otherwise stabilize the desired product complexes in the W^{IV} and W^{VI} oxidation states. Schemes 1 and 2 separately display reactions involving these groups.

By means of reaction 1 with NaSR, thiolate complexes **3** and **4** were obtained in ca. 60% yield. However, reactions with LiSeR afforded the green monocarbonyls **8** (65%) and **9** (27%) rather than the desired $n = 2$ complexes. This problem was addressed by means of reaction 2 (Q = Se), which afforded the red-orange selenolate complexes **5** (72%), **6** (72%), and **7** (65%).

$$[W(O_2CBu^t)(S_2C_2Me_2)_2]^- + RQSiMe_3 \rightarrow [W(QR)(S_2C_2Me_2)_2]^- + Bu^tC(O)OSiMe_3 \quad (2)$$

Complex **3** (53%) was also prepared by an analogous procedure (Q = S). Structures of thiolate complex **3** and selenolate complex **5** with the same R substituent are compared in Figure 2 together with the structure of **6**; metric data for **3**−**7** are collected in Table 4. The complexes are isostructural and apart from the 0.12−0.14 Å difference in W−Q axial bond lengths are essentially isometric. They adopt a square-pyramidal geometry with the tungsten atom displaced 0.70−0.75 Å toward the axial ligand and the planar chelate rings disposed at dihedral angles of 129−132°. With these and earlier examples, it is evident that this stereochemistry, with idealized C_{4v} symmetry of the WS_4Q coordination unit, is generic to $[M^{IV}L(S_2C_2R_2)_2]^z$ complexes.

(b) Decomposition Products. In a qualitative examination of stability under ambient anaerobic conditions, significant differences were found between thiolate and selenolate complexes with R = Bu^t and 1-Ad. A solution of **4** in acetonitrile was completely stable for at least 1 week, whereas **3** in this solvent showed some decomposition at 3 h and was fully decomposed within 3 days. The isolated

(36) Beswick, C. L.; Schulman, J. M.; Stiefel, E. I. *Prog. Inorg. Chem.* **2004**, *52*, 55−110.

Scheme 1. Preparative Routes to Bis(dithiolene)tungsten(IV−VI) Thiolate and Selenoate Complexes with *tert*-Butyl Substituents, Based on Dicarbonyl Complex **1** and Carboxylate Complex **2**

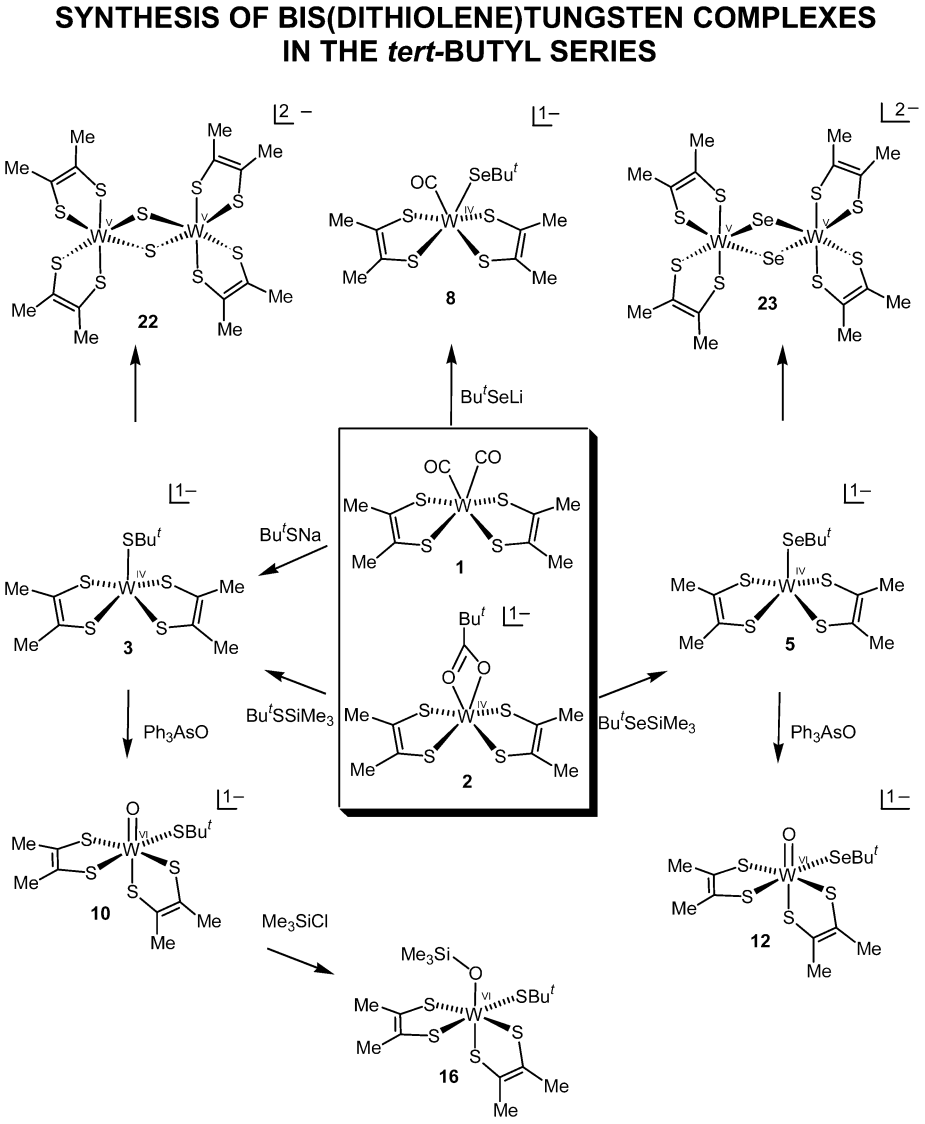

product was the doubly sulfido-bridged W^V dimer **22** (Scheme 1), demonstrated by an X-ray structure determination. $(Et_4N)_2$[**22**] (41%) was obtained from the reaction of **1** and $(Et_4N)(SBu^t)$ in acetonitrile after 3 days. For selenolate complex **5** in acetonitrile, decomposition is even faster, being complete in 1 day. The isolated product is the analogous selenido-bridged dimer **23**, identified by a structure determination (Figure 3). The complex was obtained in 77% yield after 20 h in acetonitrile. Complexes **22** and **23** are diamagnetic and isostructural (Table 5) and exhibit W···W separations too long for direct metal−metal interaction. The present structure of **22** is a polymorph of the structure of triclinic $(Et_4N)_2$[**22**]·MeCN described elsewhere.[29] In earlier work, the related complex $[W_2(\mu_2\text{-}S)_2(S_2C_2Ph)_4]^{2-}$ has been obtained by a different procedure,[34] and **22** was prepared by the iodine oxidation of $[WS(S_2C_2Me_2)_2]^{2-}$.[29] Dimers **22** and **23** must arise from cleavage of C−Q bonds with concomitant metal oxidation, as in the overall process $2RQ^- + 2e^- \rightarrow 2Q^{2-} + R-R$. Apparent precedents are found in the reactions of W^V compounds with a thiolate or selenolate that lead to products with $W^{VI}=Q$ terminal groups.[37−39]

Attempts to prepare selenolate complexes **5** and **6** by decarbonylation of the monocarbonyls **8** and **9**, respectively, under conditions of heating of acetonitrile solutions at 50 °C or allowing them to stand overnight, led to decomposition. The product isolated from **8** is the dinuclear monoanion **24** of idealized C_2 symmetry (Figure 3 and Table 4). This complex includes two dithiolene chelate rings and is bridged by one μ_2-selenium atom and two sulfur atoms from dithiolene ligands. The dithiolene bridging mode has been previously observed in $[Mo_2O(S_2C_2Me_2)_4]^-$;[22] we are unaware of a previous example of a $W^{IV}W^V$ mixed-valent dimer.

Molybdenum(IV) Sulfido Complex. Because of the possible intervention of a five-coordinate Mo^{IV}−SH/OH site in *E. coli* FDH_H (Figure 1), the unprotonated version **21** of the sulfide species was sought. This complex was obtained

(37) Kawaguchi, H.; Tatsumi, K. *J. Am. Chem. Soc.* **1995**, *117*, 3885−3886.
(38) Kawaguchi, H.; Yamada, K.; Lang, J.-P.; Tatsumi, K. *J. Am. Chem. Soc.* **1997**, *119*, 10346−10358.
(39) Kawaguchi, H.; Tatsumi, K. *Chem. Commun.* **2000**, 1299−1300.

Scheme 2. Preparative Routes to Bis(dithiolene)tungsten(IV−VI) Thiolate and Selenoate Complexes with 1-Adamantyl Substituents, Based on Dicarbonyl Complex **1** and Carboxylate Complex **2**

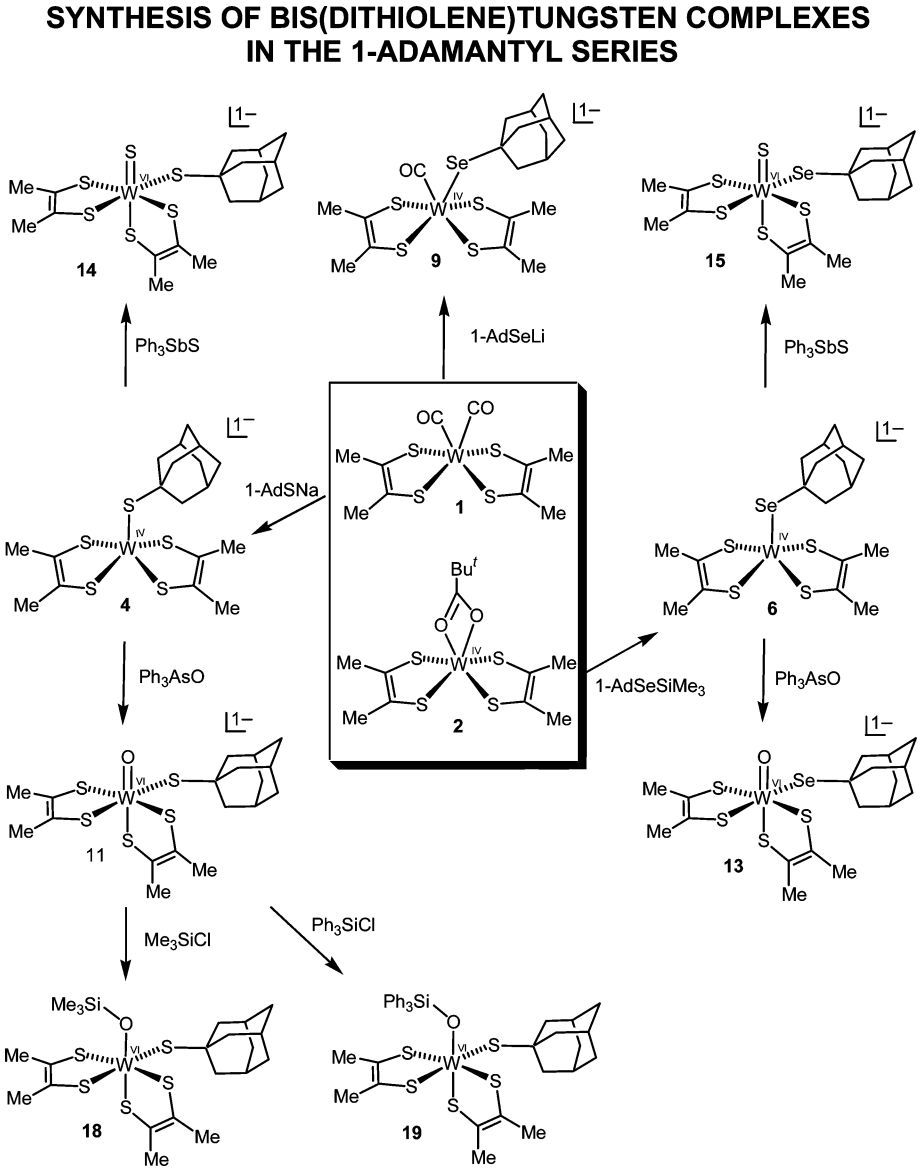

by the reaction of $[Mo(CO)_2(S_2C_2Me_2)_2]$[28] with hydrosulfide in acetonitrile and obtained in 74% yield. The compound $(Et_4N)_2$[**21**]·MeCN contains two inequivalent anions of essentially identical dimensions in the asymmetric unit. The structure of one anion is included in Figure 2. The square-pyramidal complex is isostructural with $[MoO(S_2C_2Me_2)_2]^{2-}$ [28] and $[WS(S_2C_2Me_2)_2]^{2-}$, which was prepared earlier by an analogous reaction,[29] and is characterized by an axial Mo−S bond length of 2.172(2) Å (Table 3). $[MoS(S_4)_2]^{2-}$ [40] and $[MoS(CS_4)_2]^{2-}$ [41,42] are the only examples of mononuclear Mo^{IV} complexes with multiply bonded Mo═S units.

Tungsten(VI) Complexes. (a) Oxo/Sulfido. As shown in Schemes 1 and 2, all $W^{VI}O$ and $W^{VI}S$ complexes are prepared from W^{IV} precursors by the generalized atom transfer reaction 3. Dark-purple oxothiolate complexes **10** (93%) and **11** (84%) are produced by the reaction of **3** and **4**, respectively, with a slight excess of XO = Ph_3AsO, an oxo donor of broad utility.[21,43] Gray-blue oxoselenolate complexes **12** (47%) and **13** (53%) are prepared from **5** and **6**, respectively, in a similar manner but in substantially lower yields.

$$[W(QR)(S_2C_2Me_2)_2]^- + XO/X'S \rightarrow [WO/S(QR)(S_2C_2Me_2)_2]^- + X/X' \quad (3)$$

Analogous reactions of **4** and **6** with X′S = Ph_3SbS afford the dark-violet sulfidothiolate complex **14** (89%) and gray-blue sulfidoselenolate complex **15** (43%), respectively. We have previously demonstrated the efficacy of Ph_3AsS as a sulfido transfer reagent in the preparation of $[MS(OR)(S_2C_2Me_2)_2]^-$ complexes.[21] Ph_3SbS has been little utilized in this regard but is a stronger sulfido donor than

(40) Draganjac, M.; Simhon, E.; Chan, L. T.; Kanatzidis, M.; Baenziger, N. C.; Coucouvanis, D. *Inorg. Chem.* **1982**, *21*, 3321−3332.
(41) Coucouvanis, D.; Draganjac, M. *J. Am. Chem. Soc.* **1982**, *104*, 6820−6822.
(42) Coucouvanis, D.; Draganjac, M.; Koo, S. M.; Toupadakis, A.; Hadjikyriacou, A. *Inorg. Chem.* **1992**, *31*, 1186−1196.
(43) Holm, R. H.; Donahue, J. P. *Polyhedron* **1993**, *12*, 571−589.

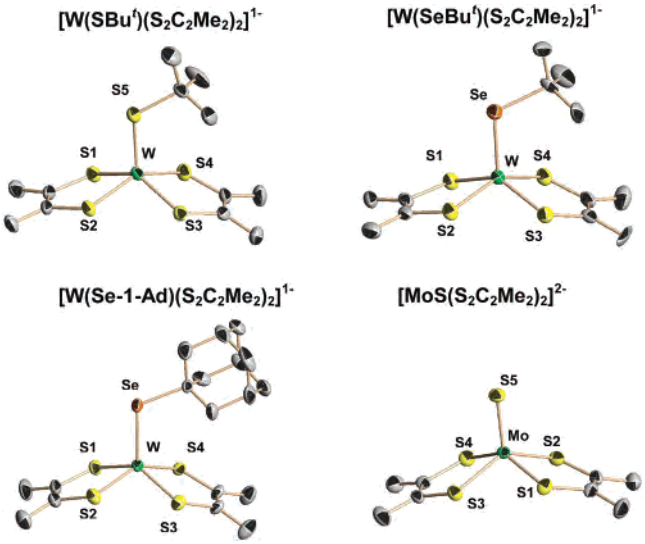

Figure 2. Structures of square-pyramidal tungsten(IV) thiolate and selenolate complexes and a molybdenum(IV) sulfido complex showing partial atom labeling schemes and 50% probability ellipsoids: upper, **3** and **5**; lower, **6** and **21**.

Ph_3AsS inasmuch as it will transfer sulfur to Ph_3As and Ph_2MeAs.[44,45] An extensive compilation of sulfur transfer agents has recently been presented by Donahue.[46]

Complexes **10** and **11** are precedented only by $[WO(SAr)(S_2C_2Me_2)_2]^-$, and **14** is precedented only by $[WS(SAr)(S_2C_2Me_2)_2]^-$, both with a very large substituent (Ar = 2,4,6-Pr$^i_3$C$_6$H$_2$)[20] to promote stability. Selenolate complexes **12**, **13**, and **15** are the first examples of the general type $[W^{VI}Q(SeR)(S_2C_2R'_2)_2]^-$ (Q = O, S). The structures of **10**−**12** are set out in Figure 4; metric parameters are collected in Table 6. They are essentially isostructural with one another and with $[WO(OPh)(S_2C_2Me_2)_2]^-$, the structure of which has been described.[47] Complexes **10** and **12** provide another comparison of thiolate and selenolate molecules at parity of the R substituent. The three molecules have an irregular six-coordinate stereochemistry with cis oxo and QBu^t ligands, an oxo trans effect of 0.09 Å, S−W−S transoid angles of 156−158°, and WS_2 dihedral angles of 93−96°. For octahedral/trigonal-prismatic stereochemistry, these angles are 180°/136° and 90°/120°. In approximate terms, the structures may be described as intermediate between these two limits. The structures of sulfidothiolate and sulfidoselenolate complexes were not determined. Diffraction-quality crystals of (Et$_4$N)[**14**] could not be obtained. Attempts to obtain suitable crystals of (Et$_4$N)[**15**] from acetonitrile/ether instead afforded crystals of the decomposition product (Et$_4$N)$_2$[**22**]. However, the proven isostructural relationship of $[WQ(SAr)(S_2C_2Me_2)_2]^-$ (Q = O, S)[20] is entirely probable for the 1-Ad complexes **11**, **14**, and **15**.

(b) Desoxo. As seen in Figure 1, a number of active site structures are proposed to contain coordinated hydroxyl, a precedented but not entirely common mode of ligation in high-valent synthetic complexes owing to the possible reaction 2M−OH → M−O−M + H_2O. In the present context, M−OH groups (M = Mo, W) are protonated versions of the oxo group M=O. In this and earlier work, we have not been able to isolate molecules containing the group M^{IV-VI}−OH derived from species with one M=O group. Examples are restricted to the monoprotonation of certain trioxo complexes to afford $[LMO_2(OH)]^{1+,0}$ (L = Bu$^t_3$tach, Me$_3$tacn;[48−50] Tp*[51]), which have been isolated and structurally characterized. Electrophiles can attack dithiolene complexes at a chelate ring sulfur atom or a multiply bonded ligand.[34,52] However, silyl reagents react exclusively at $M^{IV}O$ or $W^{VI}O_2$ groups.[53−55] As a first step, reaction 4 was investigated with $[WO(SAr)(S_2C_2Me_2)_2]^{1-}$ and Me_3SiCl. Under optimized conditions, red-brown **17** (45%) was obtained. The reaction was accompanied by the formation of two byproducts. The tris(dithiolene) complex $[W(S_2C_2Me_2)_3]$[56,57] was identified by an ^{1}H NMR spectrum and a crystal structure (not shown), and the bis(thiolate)bis(dithiolene) complex **20** was identified by a structure determination (Figure 5 and Table 6). The latter, with cis thiolate ligands, is formally related by a one-electron

$$[WO(SR)(S_2C_2Me_2)_2]^- + R'_3SiCl \rightarrow [W(OSiR'_3)(SR)(S_2C_2Me_2)_2] + Cl^- \quad (4)$$

oxidation to similarly configured $[W(QPh)_2(S_2C_2Me_2)_2]^{1-}$, whose structures have been described.[29] Oxothiolate complexes **10** and **11** in reaction 4 afford the neutral complexes **16** (33%), **18** (52%), and **19** (39%) in moderate yield. The structure of **19** (Figure 5 and Table 6) features mutually cis thiolate and silyloxide ligands and, based on a trans angle of 167°, approaches a (distorted) octahedral limit. Complexes **16**−**19**, although stable enough to isolate, tend to decompose even in a nonpolar solvent such as toluene, forming $[W(S_2C_2Me_2)_3]$ among other products. They have no precedents among bis(dithiolene) complexes. Attempts to prepare the corresponding selenolate complexes by silylation of **12** or **13** were unsuccessful. The only product identified from these reactions was the tris(dithiolene).

Comparative Features. The results described here constitute the first concerted investigation of bis(dithiolene)

(44) Baechler, R. D.; Stack, M.; Stevenson, K.; Van Valkenburgh, V. *Phosphorus, Sulfur Silicon Relat. Elem.* **1990**, *48*, 49−52.
(45) Capps, K. B.; Wixmerten, B.; Bauer, A.; Hoff, C. D. *Inorg. Chem.* **1998**, *37*, 2861−2864.
(46) Donahue, J. P. *Chem. Rev.* **2006**, *106*, 4747−4783.
(47) Sung, K.-M.; Holm, R. H. *J. Am. Chem. Soc.* **2001**, *123*, 1931−1943.
(48) Schreiber, P.; Wieghardt, K.; Nuber, B.; Weiss, J. *Polyhedron* **1989**, *8*, 1675−1682.
(49) Schreiber, P.; Wieghardt, K.; Nuber, B.; Weiss, J. *Z. Anorg. Allg. Chem.* **1990**, *587*, 174−192.
(50) Partyka, D. V.; Staples, R. J.; Holm, R. H. *Inorg. Chem.* **2003**, *42*, 7877−7886.
(51) Eagle, A. A.; George, G. N.; Tiekink, E. R. T.; Young, C. G. *Inorg. Chem.* **1997**, *36*, 472−479.
(52) Sellman, D.; Wemple, M. W.; Donaubauer, W.; Heinemann, F. W. *Inorg. Chem.* **1997**, *36*, 1397−1402.
(53) Lorber, C.; Donahue, J. P.; Goddard, C. A.; Nordlander, E.; Holm, R. H. *J. Am. Chem. Soc.* **1998**, *120*, 8102−8112.
(54) Donahue, J. P.; Goldsmith, C. R.; Nadiminti, U.; Holm, R. H. *J. Am. Chem. Soc.* **1998**, *120*, 12869−12881.
(55) Musgrave, K. B.; Lim, B. S.; Sung, K.-M.; Holm, R. H.; Hedman, B.; Hodgson, K. O. *Inorg. Chem.* **2000**, *39*, 5238−5247.
(56) Schrauzer, G. N.; Mayweg, V. P. *J. Am. Chem. Soc.* **1966**, *88*, 3235−3242.
(57) Fomitchev, D. V.; Lim, B. S.; Holm, R. H. *Inorg. Chem.* **2001**, *40*, 645−654.

Table 4. Selected Structural Data (Å, Deg) for Square-Pyramidal W^{IV} and Mo^{IV} Complexes **3**−**7** and **21**

	3	4	5	6	7	21
W/Mo−S[a]	2.314(6)	2.316(2)	2.311(4)	2.310(4)	2.311(3)	2.362(7)
W/Mo−Q_{ax}[b]	2.303(2)	2.296(1)	2.425(2)	2.434(2)	2.435(1)	2.172(2)
S−C[c]	1.77(1)	1.768(5)	1.77(2)	1.76(1)	1.77(1)	1.774(3)
C−C[c]	1.33(1)	1.327	1.34(2)	1.33(1)	1.32(1)	1.341(6)
δ[d]	0.718	0.707	0.701	0.746	0.728	0.815
θ[e]	131.2	132.2	132.4	129.2	130.5	125.7

[a] Mean values. [b] Q = S (**3**, **4**, **21**), Se (**5**−**7**). [c] Chelate ring. [d] Perpendicular displacement of a tungsten atom from the S_4 least-squares plane. [e] Dihedral angle between WS_2 planes.

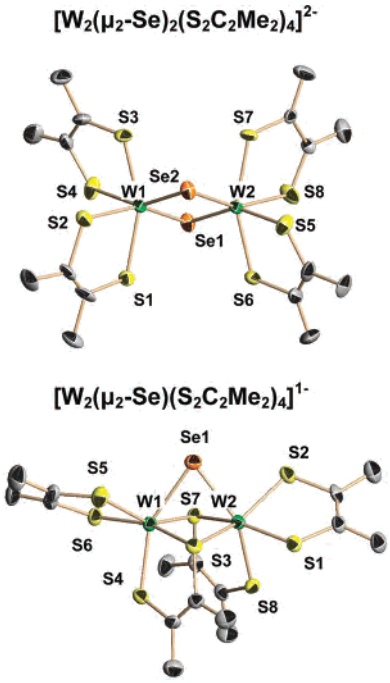

Figure 3. Structures of selenide-bridged dinuclear tungsten complexes showing partial atom labeling schemes and 50% probability ellipsoids: upper, **23**; lower, **24**. The structure of **22** (not shown) is commensurate with that of **23**.

Table 5. Selected Structural Data for Dinuclear Complexes **22**−**24**

	22	23	24
W−S[a]	2.41(2)	2.41(2)	2.36(1)
W−(μ_2-Q)[a,b]	2.327(4)	2.45(2)	2.49(1)
W−(μ_2-SR)[a]			2.47(2)
W−W	2.989(1)	3.111(4)	2.868(1)
S−C[a]	1.74(1)	1.75(3)	1.76(1)
C−C[a]	1.340(1)	1.36(4)	1.34(1)
W−Q−W[b]	79.92(5)	78.5(1)	70.38(2)
S−W−S[c]	156.58(7)[c]	156.6(1)[a]	
S−W−Q[a,b,c]	155.5(3)	156(1)	

[a] Mean values. [b] Q = S (**22**), Se (**23**, **24**). [c] Transoid angle.

selenolate complexes of any type and, in particular, those related in varying degrees to FDH active sites. Here we compare certain related features of bis(dithiolene) complexes in terms of metal and ligand and the structures of these complexes and enzyme sites.

(a) Molybdenum vs Tungsten. As noted earlier, tungsten complexes were prepared because of the autoredox instability of Mo^{VI} complexes containing electron-rich dithiolene ligands.[58] Molybdenum and tungsten complexes at strict parity of oxidation state and ligation manifest certain differences and similarities. Among the differences are the potential order $E_W < E_{Mo}$ for a given redox couple,[59]

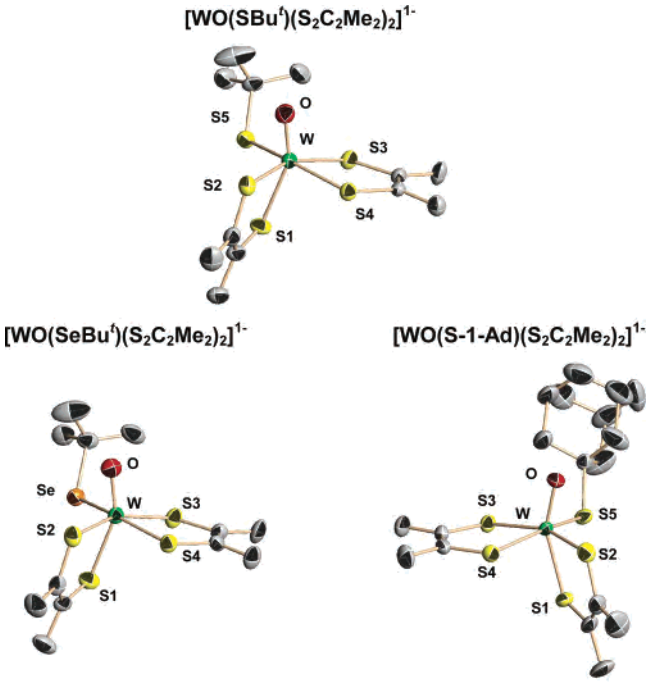

Figure 4. Structures of tungsten(VI)−oxothiolate and selenoate complexes showing partial atom labeling schemes and 50% probability ellipsoids: upper, **10**; lower, **11** and **12**.

Table 6. Selected Structural Data (Å, Deg) for W^{VI} Complexes **10**−**12**, **19**, and **20**

	10	11	12	19	20
W−S1	2.501(2)[a]	2.497(1)[a]	2.495(2)[a]	2.408(1)	2.378(2)
W−S2	2.382(2)	2.383(1)	2.373(2)	2.383(1)	2.357(2)
W−S3	2.406(2)	2.406(1)	2.406(2)	2.364(1)	2.378(2)
W−S4	2.437(2)	2.424(1)	2.427(2)	2.403(1)	2.387(2)
W−Q[b]	2.435(2)	2.416(1)	2.564(1)	2.351(1)	2.368(9)[c]
W−O	1.717(6)	1.741(3)	1.729(6)	1.861(3)	
S−C[d]	1.74(2)	1.74(3)	1.72(2)	1.73(2)	1.71(2)
C−C[d]	1.35(1)	1.34(1)	1.33(1)	1.337(7)	1.36(1)
O−W−S1	155.4(2)	154.9(1)	155.1(2)	156.9(1)	
O−W−Q[b]	93.8(2)	95.2(1)	93.2(2)	97.8(1)	
S2−W−S3[e]	155.93(8)	158.48(4)	156.55(8)	167.40(5)	153.37(8)[f]
S4−W−Q[b,e]	160.33(7)	157.78(4)	160.39(5)	154.48(5)	
θ[g]	95.2	93.5	96.4	91.6	59.0

[a] Trans to oxo. [b] Q = S(R) (**10**, **11**, **19**), Se(R) (**12**). [c] Mean of W−S5/S6. [d] Chelate ring. [e] Transoid angle. [f] Respective angles for S1−W−S4 and S2−W−S5 are 139.06(9)° and 143.84(8)°. [g] Dihedral angle between WS_2 planes.

illustrated by the $M^{IV/V}$ potentials in acetonitrile for isostructural oxo and sulfido complexes, including **21**. The very

(58) A limited set of bis(dithiolene)molybdenum(VI) complexes have been isolated with use of the more electronegative ligands bdt[54,64,65] and mnt.[66] These ligands are less accurate representations of the chelate portion of the pyranopterindithiolene cofactor ligand.

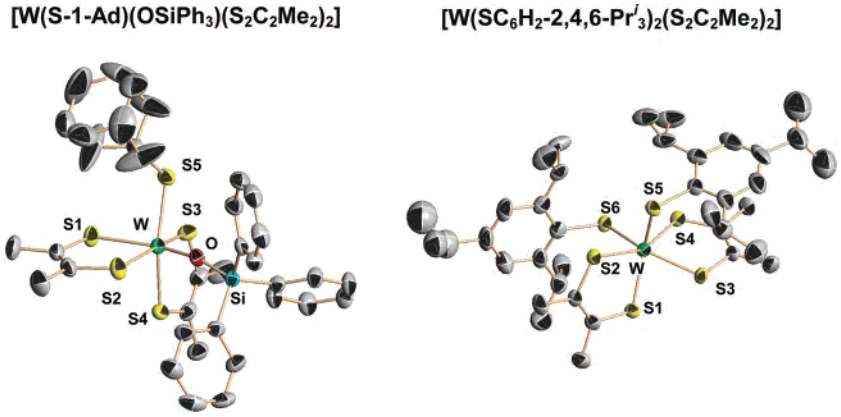

Figure 5. Structures of desoxo/sulfido tungsten(VI) complexes showing partial atom labeling schemes and 50% probability ellipsoids: right, **19**; left, **20**.

small dependence on the axial ligand Q (20−30 mV) follows from the symmetry-restricted interactions between the electroactive d_{xy} orbital and the filled s and p valence orbitals of

$[MO(S_2C_2Me_2)_2]^{2-}$ M = Mo (−0.62 V),[28] W (−0.91 V)[34]

$[MS(S_2C_2Me_2)_2]^{2-}$ M = Mo (−0.65 V), W (−0.89 V)[29]

Q. A further difference is the rate constant order of $k_W > k_{Mo}$ for oxo transfer from substrate to metal and of $k_{Mo} > k_W$ for the reverse process.[21,47,59,60] The most significant similarity is a virtual identity: pairs of molybdenum and tungsten complexes are isostructural and nearly isometric. There are no exceptions. For example, in the six comparative pairs of complexes $[MQ(S_2C_2Me_2)_2]^{2-}$ [28,34] and $[M(QR)(S_2C_2Me_2)_2]^-$ [20,26−28] (Q = O, S) and $[M(OSiR_3)(bdt)_2]^-$ and $[MO(OSiR_3)(bdt)_2]^-$,[53,54] differences in mean M−S distances in chelate rings are ∼0.01 Å, in M−Q distances ∼0.04 Å, and in M−OSi distances ∼0.02 Å. Bond angles also display very little variation. Under the foregoing stricture, tungsten is a structural surrogate of molybdenum.

(b) Selenium vs Sulfur. In the present work, the most important difference is that selenolate complexes are clearly less stable than thiolate complexes in solution, as documented above. The UV−vis spectra of dithiolene complexes are generally dominated by ligand-to-metal charge transfer absorptions involving dithiolene ligand orbitals with significant sulfur character.[61] All complexes prepared in this work are intensely colored and exhibit such spectra. Among them, pairs differing only in a selenium vs sulfur donor atom show a systematic behavior in which all or nearly all of the transitions in the selenolate complex are shifted to lower energies. The effect is particularly clear in the 1-Ad complexes comprising the W^{IV} pair **4**/**6** and the W^{VI} pair **14**/**15**, whose spectra are shown in Figure 6. Spectral shifts are those expected based on the optical electronegativity order Se < S, but band assignments are required for an

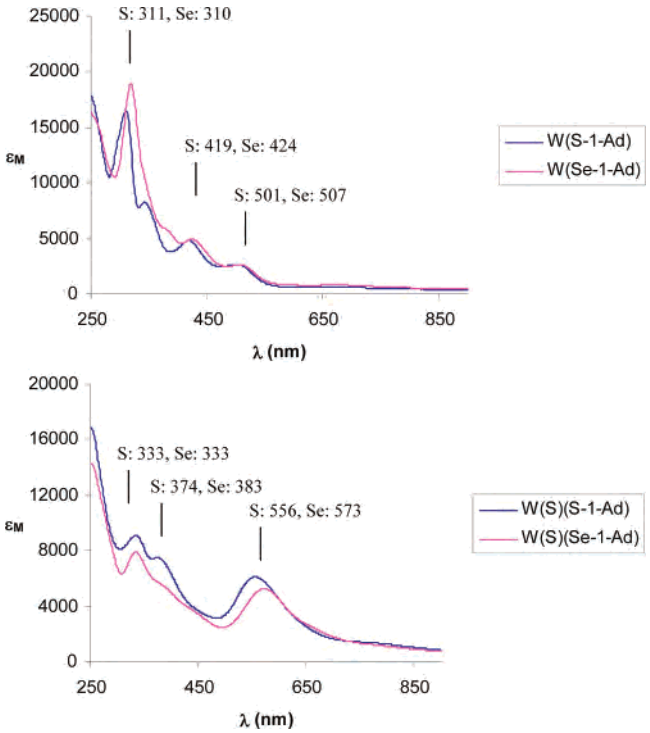

Figure 6. Comparative UV−vis absorption spectra of pairs of $[W(QR)(S_2C_2Me_2)_2]^-$ and $[WS(QR)(S_2C_2Me_2)_2]^-$ complexes (Q = S, Se) in acetonitrile; λ_{max} values are indicated: upper, **4** and **6**; lower, **14** and **15**.

evaluation of the origin of the shifts. A similar but less clearly displayed effect is found in the series $[Mo(Q\text{-}2\text{-}Ad)(S_2C_2Me_2)_2]^-$ (Q = O, S, Se).[26] In the absence of crystal structures, the spectra of **14** and **15** serve as characterization information.

(c) Synthetic Complexes and Enzyme Sites. With reference to Figure 1 and Table 3, $[Mo(Se\text{-}2\text{-}Ad)(S_2C_2Me_2)_2]^-$ and selenolate complexes **5**−**7** are analogues of the originally described square-pyramidal formate-reduced site of *E. coli* FDH_H,[7] and $[Mo(SR)(S_2C_2Me_2)_2]^-$, **3**, **4**, and $[W(SAr)(S_2C_2Me_2)_2]^-$ are their thiolate counterparts. Complex **21** is an unprotonated form of the revised description of the formate-reduced site without selenocysteinate binding.[8] Complexes **12** and **13** are unprotonated versions of the oxidized sites of *E. coli* FDH_H and FDH_N and *D. gigas* W−FDH with bound hydroxyl, and **10**, **11**, and

(59) Tucci, G. C.; Donahue, J. P.; Holm, R. H. *Inorg. Chem.* **1998**, *37*, 1602−1608.
(60) Jiang, J.; Holm, R. H. *Inorg. Chem.* **2005**, *44*, 1068−1072.
(61) Kirk, M. L.; McNaughton, R. L.; Helton, M. E. *Prog. Inorg. Chem.* **2004**, *52*, 111−212.

$[WO(SAr)(S_2C_2Me_2)_2]^-$ are their thiolate counterparts. The latter are representations of the oxidized site of a mutant FDH that is ca. 300 times less active than the wild-type enzyme.[62] Complex **15** simulates the unprotonated oxidized sites of *E. coli* FDH_H and *D. gigas* W−FDH with coordinated hydrosulfide, and $[WS(SAr)(S_2C_2Me_2)_2]^-$ and **14** are thiolate complements. Protonated Mo^{VI} and W^{VI} enzyme sites are desoxo/sulfido entities. Thiolate complexes **16**−**19** serve to demonstrate that desoxo complexes, at least with W^{VI}, are sufficiently stable for isolation. Here a silyloxide group mimics protonation. We have not prepared any complex related to the dithionite-reduced six-coordinate form of *D. sulfuricans* FDH deduced from EXAFS analysis. Given the structural relationship between molybdenum and tungsten complexes, the selenolate complexes are symmetrized representations of enzyme sites whose metric features are or approach those expected in the absence of the constraints imposed by protein structure. In this context, thiolate complexes serve as site representatives of the homologues of selenocysteinate proteins that contain Cys instead of SeCys at the active centers.[63]

This investigation and prior work (Table 3) demonstrate that bis(dithiolene) selenolate complexes of molybdenum and tungsten are synthetically accessible but are less stable than analogous thiolate complexes. Indeed, the isolation of both **14** and **15**, containing W^{VI} bound to anionic reducing sulfur or sulfur and selenium ligands, is notable. With this set of new complexes in hand, the binding of formate and the attainment of an FDH analogue reaction system are under investigation.

Acknowledgment. This research was supported by NSF Grants CHE 0237419 and 00547734. We thank J.-J. Wang and Dr. C. Tessier for helpful discussions.

Supporting Information Available: X-ray crystallographic files in CIF format for the structure determinations of the compounds in Tables 1 and 2. This material is available free of charge via the Internet at http://pubs.acs.org.

IC062441A

(62) Axley, M. J.; Böck, A.; Stadtman, T. C. *Proc. Natl. Acad. Sci. U.S.A.* **1991**, *88*, 8450−8454.
(63) Gladyshev, V. N. *Met. Ions Biol. Syst.* **2002**, *39*, 655−672.
(64) Ueyama, N.; Oku, H.; Kondo, M.; Okamura, T.; Yoshinaga, N.; Nakamura, A. *Inorg. Chem.* **1996**, *35*, 643−650.
(65) Sugimoto, H.; Tarumizu, M.; Tanaka, K.; Miyake, H.; Tsukube, H. *J. Chem. Soc., Dalton Trans.* **2005**, 3558−3565.
(66) Das, S. K.; Chaudhury, P. K.; Biswas, D.; Sarkar, S. *J. Am. Chem. Soc.* **1994**, *116*, 9061−9070.